A relativistic appearance of hotspots on an ultra-compact dark star

Galin Gyulchev

Faculty of Physics, Sofia University, 5 James Bourchier Boulevard, 1164 Sofia, Bulgaria

E-mail: gyulchev@phys.uni-sofia.bg

Abstract. We depict the deflection of light near ultra-compact dark energy stars with a photon sphere, drawing inspiration from modern confirmations of general relativity. Utilizing the description of dark energy through a phantom scalar field, we model the spacetime outside the star using an exact dark energy solution metric. We provide a summary of the properties of photon orbits. Additionally, we illustrate the relativistic appearance of a hot spot on the surface of a dark energy star and investigate both the optical appearance of the surface and the star's visual size on the screen of an asymptotic observer.

1. Introduction

Dark stars have become increasingly popular in the last decade due to astronomical studies involving distant supernovae, cosmic microwave background, and weak-field gravitational lensing. All of these studies have confirmed the Universe's accelerated expansion. Since dark energy constitutes a significant portion of our Universe, it is expected to interact with ordinary matter in various astrophysical manifestations such as wormholes, black holes, and exotic compact stars.

The coexistence of dark energy and ordinary matter suggests that existing stars may consist of a combination of both substances in varying proportions. Recently, realistic models of massive compact objects, including neutron and strange stars composed of high-density fluid and dark energy modeled by a scalar field interacting with matter, have been developed [1, 2, 3, 4, 5].

Some compact stars with dark energy, proposed in [6], are among the most ultra-compact objects in the universe. These stars can have a highly relativistic surface similar to that of ultra-compact neutron stars, which have a photon sphere. When light is emitted from the surface of a compact dark energy star, significant deflection can occur, especially when the star's compactness is high enough that its radius approaches that of the photon sphere. This phenomenon results in the appearance of multiple relativistic images with heightened brightness, which can replicate hot emission regions on stars for a distant observer.

There have been several studies on the deformation of images near neutron stars and black holes. These studies include works by [7, 9, 10, 11, 13, 14, 15, 16, 17]. Furthermore, Nemiroff et al. [18] also studied the properties of ultra-compact neutron stars that have a small radius and exhibit a photon sphere. Bogdanov et al. [19] proposed a method to extract the radius-to-mass ratio of a neutron star using the NICER experiment. This method is based on the relativistic gravitational lensing effect caused by highly mass-dense pulsars. Gyulchev [20] established a noticeable increase in the visual size of ultra-compact neutron stars with a photon sphere, allowing the distinction of stars with extreme surface gravity from less compact neutron stars.

Given these advancements, the study of relativistic gravitational lensing when light passes very close to massive bodies, such as ultra-compact dark energy stars, remains deserving of attention. Consequently, we will examine the visual manifestation of the surface of a dark energy star harboring a photon sphere to propose a comprehensive depiction of the influence of the dark scalar field on the multitude of relativistic images.

The paper is organized as follows: In the next section, we present the dark energy star solution. Section 3 outlines the physical compactness of the dark-energy star. Then, in Section 4, we calculate the photon sphere and consider the values of the dark charge and compactness at which the star is able to "push" its photon sphere out of its surface. In Section 5, we discuss the ray tracing algorithm and elucidate the formation of relativistic images of the hot spots. Finally, in the last section, we present our conclusions.

2. Dark-Energy Star Solution

This work studies the relativistic gravitational lensing effect by a star containing ordinary matter and dark energy. We adopt a description of the dark energy by a phantom scalar field. Then, the Einstein equations in the presence of dark energy read

$$R_{\mu\nu} = 8\pi\Big(T_{\mu\nu} - \frac{1}{2}T\,g_{\mu\nu}\Big) - 2\partial_\mu\varphi\partial_\nu\varphi, \qquad \nabla_\mu\nabla^\nu\varphi = 4\pi\rho_D. \tag{1}$$

Here $T_{\mu\nu}$ is the energy-momentum tensor of the ordinary matter in the isotropic perfect fluid description with energy density ρ and pressure p:

$$T_{\mu\nu} = (\rho + p)u_\mu u_\nu + p\,g_{\mu\nu}. \tag{2}$$

We impose the natural conditions $\rho > 0$ and $p > 0$ for the ordinary matter. The charge density of the phantom field is denoted by ρ_D, and the "dark charge" D will be the dark energy source. The phantom kinetic term is given on the second term of the right-hand side of the first Eq. (1). When considering an astrophysical scale of the manifestation of the dark energy, the phantom field's potential can be neglected [1]. It is also considered that there is no interaction between the phantom field and the ordinary matter.

The resulting exact solutions to the Einstein field equations describe mixed relativistic dark energy stars. The dark star solutions are characterized by the mass M, the dark charge D, and the coordinate radius R.

On the dark star surface and in the region outside the star $r \geq R$, the exterior solution to the Einstein equation in terms of M and D reads [1]

$$\begin{aligned} ds^2_{ext} &= -\Big(1 - \frac{2\sqrt{M^2-D^2}}{r}\Big)^{\frac{M}{\sqrt{M^2-D^2}}}dt^2 \\ &\quad +\Big(1 - \frac{2\sqrt{M^2-D^2}}{r}\Big)^{-\frac{M}{\sqrt{M^2-D^2}}}dr^2 \\ &\quad +\Big(1 - \frac{2\sqrt{M^2-D^2}}{r}\Big)^{1-\frac{M}{\sqrt{M^2-D^2}}}r^2(d\theta^2 + \sin^2\theta\,d\phi^2), \end{aligned} \tag{3}$$

$$\varphi_{ext} = \frac{D}{2\sqrt{M^2-D^2}}\ln\Big(1 - \frac{2\sqrt{M^2-D^2}}{r}\Big). \tag{4}$$

This solution reduces to the exterior Schwarzschild solutions in the absence of dark energy (i.e. for $D = 0$).

3. The Compactness of the Dark-Energy Star.

If the pressure condition $p(R) = 0$ is satisfied, R can be interpreted as the coordinate radius of the star. Hence, the physical radius of the star, as a function of the dark charge per mass, $d = D/M$, reads

$$\mathcal{R}_{ph} = R\left(1 - \frac{2M}{R}\sqrt{1-d^2}\right)^{-\frac{1-\sqrt{1-d^2}}{2\sqrt{1-d^2}}}. \tag{5}$$

For given compactness of the star $\kappa = M/R$, we define the physical compactness as follows

$$\kappa_{ph} = \frac{M}{\mathcal{R}_{ph}} = \kappa\left(1 - 2\kappa\sqrt{1-d^2}\right)^{\frac{1-\sqrt{1-d^2}}{2\sqrt{1-d^2}}}. \tag{6}$$

The spacetime within the dark-energy star is completely regular everywhere for $0 \leq r \leq R$ if the coordinate R satisfy the inequality [1]

$$\frac{\sqrt{M^2 - D^2}}{R} < \frac{4}{9}, \tag{7}$$

which for $d < 1$ in the non extremal dark star configuration gives a limitation for the compactness at a given dark charge

$$\kappa < \frac{4}{9\sqrt{1-d^2}}. \tag{8}$$

In this study we are not going to consider a relativistic appearance of the surface of an extremal ultracompact dark-star when $d = 1$.

4. Photon Sphere

To study the capability of the dark energy star to create relativistic images, we solve the photon sphere equation [23]

$$g_{tt}(r)g'_{\theta\theta}(r) - g_{tt}(r)g'_{\theta\theta}(r) = 0, \tag{9}$$

which for the studied static and spherically-symmetric metric in the equatorial plane possesses a solution

$$r_{ps} = \left(2 + \sqrt{1-d^2}\right)M. \tag{10}$$

Of particular interest to our consideration will be the study of the visual features of the stellar surface at sufficiently large compactness when the photon sphere is located outside the surface of the star. It is important to note that higher compactness is needed to observe relativistic effects in stars with large values of the dark charge, for which the photon sphere is more compact than those in zero dark charge scenarios.

5. Ray-Tracing and Relativistic images of hot spots.

We are using backward numerical ray tracing to track the path of photons emitted from the observer's position and hitting the surface of a star with a unit radius $\mathcal{R}_{ph} = 1$. For convenience, we use two celestial coordinates to describe the projection of the light rays on the observer's sky. As suggested in [21], we introduce two angles: γ, which ranges from 0 to π, and δ, which ranges from $-\pi/2$ to $\pi/2$. For a static and spherically symmetrical spacetime, these angles are related to the photon's 4-momentum as follows:

$$\begin{aligned} p_t &= -E = -\sqrt{-g_{tt}}, & p_\varphi &= L_z = \sqrt{g_{\varphi\varphi}}\,\sin\delta\,\cos\gamma, \\ p_r &= \sqrt{g_{rr}}\,\cos\delta\,\cos\gamma, & p_\theta &= \sqrt{g_{\theta\theta}}\,\sin\gamma. \end{aligned} \tag{11}$$

We assume that the observer is located in the asymptotically flat part of the spacetime at a distance r_{obs} from the dark star. For a fixed inclination angle θ_{obs} of the observer, the angles (γ, δ) determine unique values of the photon's angular momentum and energy, allowing us to parameterize each photon trajectory unambiguously. We can describe the image created from a single photon using Bardeen's coordinates for that distant observer [22], defined as follows:

$$\alpha = -\frac{L_z}{\sin\theta_{obs}}, \qquad \beta = p_\theta. \tag{12}$$

In Figure 1, the apparent images of hot spots on a dark energy star in the observer's plane (α, β) are presented for various values of the scaled dark charge d and compactness κ. After positioning the observer at an inclination angle defined by $\theta_{obs} = \pi/3$ and a distance of $r_{obs} = 200M$, the angles γ and δ determine the impact parameters (α, β) via the initial photon momenta, (11). With these initial conditions, photons evolve backwards in time until they encounter the surface of the dark star. To interpret the resulting gravitational lensing patterns, we partition the surface of the star into multiple quadrants, each with an angular width of 30°, and alternate between red and blue colors.

When compared to the results within general relativity (depicted in the first row and in [20]), the presence of a phantom field in the case of the dark star diminishes the star's ability to generate relativistic images, as observed in the second and third rows. The displayed cases depict particular astrophysical interest where one of the hot spots is positioned on the optical axis, precisely behind the gravitational center of mass. In this specific scenario, the hot spot, acting as a light source, emits photons that, during their propagation, wind around the star's photon sphere multiple times before reaching the observer. If the conditions for this phenomenon were present, a distant observer would perceive a superposition of multiple relativistic Einstein rings symmetrically arranged around the center of the star.

On the other hand, for relatively small values of the scaled dark charge, the star can still produce relativistic hot spot images from the stellar surface, especially at relatively large values of the compactness parameter. Moreover, with larger compactness, the size of the photon sphere increases, significantly boosting the brightness and broadening the integral width of the set of relativistic rings. In contrast, as the scaled dark charge increases, the star's considerable compactness diminishes its ability to form an off-surface photon sphere. This property prevents the star from generating relativistic images of its entire surface; thus, relativistic images of the hot emission regions of interest in the present study cannot be formed. It is for this reason that dark stars possessing a larger charge density of the phantom field cannot produce relativistic images of their surface, even at large compactness.

6. Conclusion

In this paper, we investigate the observational characteristics of ultracompact stars mixed with dark energy. Modeling the star as a compact object with a relatively high dark energy density, we have found that these strange stars can be distinguished only faintly in their observational characteristics from stars in general relativity, even at significant compactness. Conversely, relativistic effects in these dark stars can become perceptible to a distant observer at small and medium values of the dark energy density. This phenomenon, coupled with sufficiently large compactness, leads to the formation of a photon sphere above the star's surface and thus multiple relativistic Einstein rings imaging the hot spots. It is precisely due to these parameter dynamics that dark stars can be much more challenging to detect observationally, as their surface brightness images are smaller in magnitude compared to those of general relativity in the absence of a dark scalar field.

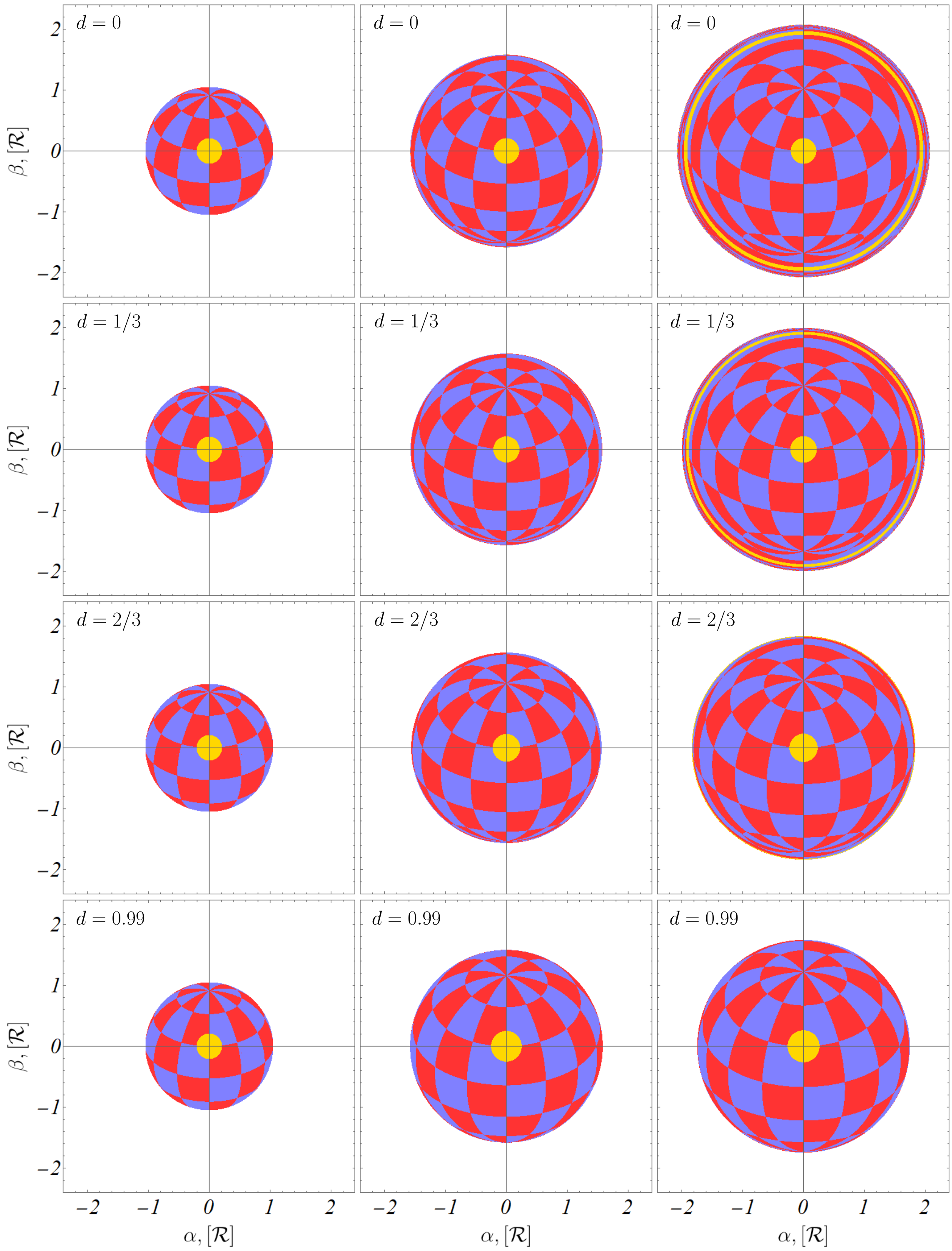

Figure 1. Image sequence of a neutron star with spherical coordinate grid for compactness $\kappa = 0$ (*left column*), $\kappa = 0.294$ (*central column*) and $\kappa = 0.4$ (*right column*) and scaled dark charge $d = 0$ (*first row*), $d = 1/3$ (*second row*), $d = 2/3$ (*third row*) and $d = 0.99$ (*fourth row*). The observer is located on a distance $r_{obs} = 200M$ as the inclination angle with respect to the north pole of the star is $\theta_{obs} = 60°$.

7. Acknowledgements

The author gratefully acknowledges support by the Bulgarian National Science Fund Grant KP-06-H62/6 from 15.12.2022.

References

[1] Stoytcho S. Yazadjiev, Exact dark energy star solutions, Phys. Rev. D 83, 127501 (2011).
[2] P. Beltracchi and P. Gondolo, Formation of dark energy stars, Phys. Rev. D 99, 044037 (2019).
[3] Mafa Takisa, P., Leeuw, L.L. and Maharaj, S.D. Model of compact star with ordinary and dark matter. Astrophys Space Sci 365, 164 (2020). https://doi.org/10.1007/s10509-020-03878-3
[4] Muhammad F. A. R. Sakti and Anto Sulaksono, Dark energy stars with a phantom field, Phys. Rev. D 103, 084042 (2021).
[5] M.Malaver, H.D.Kasmaei, R.Iyer, S.Sadhukhan, A.Kar, A theoretical model of Dark Energy Stars in Einstein-Gauss-Bonnet Gravity, https://doi.org/10.48550/arXiv.2106.09520
[6] Artyom V. Astashenok, Sergey D. Odintsov, Vasilis K. Oikonomou, Compact stars with dark energy in general relativity and modified gravity, Physics of the Dark Universe, 42, 101295 (2023), https://doi.org/10.1016/j.dark.2023.101295.
[7] F.W. Hehl, R.A. Puntigam, H. Ruder, Relativity and Scientific Computing: Computer Algebra, Numerics, Visualization, Springer, (1996).
[8] C. Fraclas, C. Kearney, M.W.K. Pechenick, Astrophys. J. **300**, 203 (1986).
[9] R. J. Nemiroff, Visual Distortions near a neutron star and black hole, *Am. J. Phys* **61**, 619-631 (1993).
[10] D. R. Wilkins, On the illumination of neutron star accretion discs, *MNRAS* **475**, 1, 748–756 (2018).
[11] G. A. Oliva, F. Frutos-Alfaro, Effects of the treatment of the mass quadrupole moment on ray-tracing applications for rapidly-rotating neutron stars, *MNRAS* **505**, 2, 2870-2885 (2021).
[12] S. Bhattacharyya, Measurement of neutron star parameters: A review of methods for low-mass X-ray binaries, *Advances in Space Research*, **45**, 8, 949-978, (2010).
[13] H.P. Nollert, H. Ruder, H. Herold and U. Krauss, The relativistic ”looks” of a neutron star, *Astronomy and Astrophysics* **208**, 1-2, 153-156 (1989).
[14] U. Krauss, Light Deflection Near Neutron Stars, *Relativistic Astrophysics*, 66-81, Vieweg+Teubner Verlag, Wiesbaden (1998).
[15] Dabrowski, M.P., Osarczuk, J. Light curves of relativistic charged neutron star. Astrophys Space Sci 229, 139–155 (1995)
[16] H. Sotani, Light curves from highly compact neutron stars with spot size effect, *Phys. Rev. D* **101**, 063013 (2020).
[17] K.R. Pechenick, C. Ftaclas and J.M. Cohen, Hot spots on neutron stars: The near-field gravitational lens, *ApJL*, **274**: 846-857 (1983).
[18] R.J. Nemiroff, P.A. Becker and K.S. Wood, Properties of ultracompact neutron stars, *ApJ* **406**: 590-595 (1993).
[19] Bogdanov et al, Constraining the Neutron Star Mass–Radius Relation and Dense Matter Equation of State with NICER. II. Emission from Hot Spots on a Rapidly Rotating Neutron Star, *ApJL* **887** L26 (2019).
[20] G.N. Gyulchev, Observational features of hot spots on neutron stars with a photon sphere, JPCS, 2255, 012005 (2022).
[21] P. Cunha, C. Herdeiro, E. Radu, H. Runarsson, Shadows of Kerr black holes with and without scalar hair. Int. J. Mod. Phys. D 25, 1641021 (2016).
[22] J. M. Bardeen, Timelike and null geodesics in the Kerr metric, in Black Holes, eds. C. DeWitt and B. DeWitt, Gordon and Breach, New York (1973) p. 215.
[23] Clarissa-Marie Claudel, K. S. Virbhadra, G. F. R. Ellis, The geometry of photon surfaces, J. Math. Phys. 42 (2): 818–838 (2001), https://doi.org/10.1063/1.1308507